STUDIA UNIVERSITATIS BABEŞ-BOLYAI BIOLOGIA, 71, 1, 2026 (p. 59-70)
doi:10.24193/subbbiol.2026.1.04

Functional study of PAP3/pTAC10 in the plastid-encoded RNA polymerase during chloroplast biogenesis

Leonard Calistru[1]✉, Florent Velay[2], Dorina Podar[1], and Robert Blanvillain[2]✉

[1]Babeş-Bolyai University; Str. Republicii nr. 44, Cluj-Napoca, Roumania; [2]CNRS, CEA, INRA, IRIG-LPCV Univ. Grenoble-Alpes Grenoble France;
✉***Corresponding authors, E-mail: leonard.calistru@gmail.com; robert.blanvillain@cea.fr***

Article history: Received 30 July 2025; Revised 24 February 2026; Accepted 30 April 2026; Available online 25 June 2026

Abstract. Chloroplast biogenesis in angiosperms depends on two types of RNA polymerases: the nuclear-encoded RNA polymerase (NEP) and the plastid-encoded RNA polymerase (PEP). PEP, in its active form (PEP-A), is supported by multiple nuclear-encoded proteins called PEP-associated proteins (PAPs). Among these, PAP3 (also known as pTAC10) plays a structural role in the PEP complex. Epifluorescent microscopy was used in order to verify its localization, confirming that PAP3 has a single subcellular localization: the chloroplast. Using the *Arabidopsis thaliana pap3-1* mutant and PHYB-GFP (PBG) reporter lines, we demonstrate that PAP3 is not required for PHYB-mediated light signaling pathway nor for photobody formation. Contrary to PAP8, whose loss of function affects red light signaling and photobody formation, *pap3* mutants show normal hypocotyl de-etiolation and photobody assembly under red light. These results suggest that in contrast with the nucleo-chloroplastic PAP8, PAP3 is confined to the plastid compartment and that it contributes exclusively to the plastidial transcriptional machinery. The difference in behavior between *pap8* and *pap3* mutants implements the existence of two distinct albino syndromes in PAPs, depending on their localization: dually localized (nucleus and chloroplasts) or solely localized (chloroplasts).

Keywords: chloroplast biogenesis, PAP3, photobodies, phytochrome B, plastid-encoded RNA polymerase.

Introduction

Plastids are cell organelles that are at the main sites of photosynthesis in eukaryotic cells. Their origin traces back to an event in which a cyanobacteria-like photosynthetic prokaryote was engulfed by a mitochondriated eukaryotic cell, resulting in a stable endosymbiosis of mutual benefit (Archibald, 2015). Within a multicellular photosynthetic organism, plastids can be divided based on their color, morphology, and ultrastructure into several types, such as: proplastids, chromoplasts or chloroplasts (Choi *et al.*, 2021).

The chlroplast has a much-reduced genome compared to its cyanobacterial ancestors because most of its genes were transfered to the nucleus of the eukaryotic cell following the primary endosymbiosis (Bock and Timmis, 2008). In order to accommodate these changes, plastid genes are transcribed by two types of RNA polymerases in angiosperms: the bacterial type plastid-encoded RNA polymerase (PEP) and one (RPOTp in monocots) or two (RPOTp and RPOTmp in dicots) nuclear-encoded RNA polymerase(s) (NEP) (Börner *et al.*, 2015). This division of labor between NEP and PEP allowed plants to regulate efficiently plastid gene expression under diverse conditions. While PEP transcribes photosynthesis-related genes, NEP alone transcribes a few housekeeping genes (Börner *a.*, 2015).

PEP exists in two forms: PEP-A and PEP-B. PEP-B is the low-active prokaryotic–like catalytic core enzyme composed of the α, α, β, β′, and β′′ subunits encoded by the plastid genes rpoA, rpoB, rpoC1, and rpoC2. The PEP-A complex consists of the catalytic core enzyme associated with nuclear-encoded additional proteins named PAPs (Steiner *et al.*, 2011; Liebers *et al.*, 2022).

PEP-associated proteins (PAPs) are structurally and functionally diverse, and can be divided based on their potential function, such as DNA/RNA metabolism, redox regulations, ROS protection, or unknown (Kindgren and Strand, 2015). Functional inactivation via T-DNA insertion in most PAP genes lead to an arrest in chloroplast biogenesis, resulting in ivory or albino plants that are only viable upon the addition of a carbon source (e.g. sucrose) in sterile growth conditions (Liebers *et al.*, 2022). Out of the 12 PAPs identified so far, six contain a predicted nuclear localization signal (NLS) according to the algorithm of cNLS mapper. Some of these PAPs, such as PAP8 or PAP5, display a nucleo-chloroplastic accumulation of the GFP-tagged proteins, meaning that they are dually localized to the nucleus and chloroplast (Liebers *et al.*, 2022).

In angiosperms, chloroplast development, perceived as an initial greening, is preceded by light activation of photoreceptors that trigger photomorphogenesis. One key photoreceptor is phytochrome-B who senses red (600-700 nm) and far-red light (700-750 nm), and triggers the transition from skotomorphogenesis (growth in the dark) to photomorphogenesis (growth in the light), promoting

the development of green chloroplasts, de-etiolation and inhibition of stem elongation (Liebers *et al.*, 2020). Phytochrome-B, alongside other phytochromes (A to E), is found in membraneless organelles called photobodies (Yoo *et al.*, 2019). Initially appearing as small, transient foci, photobodies mature into larger, more stable structures under continuous red light exposure, suggesting a functional transition from early signaling platforms to photostable repositories for active phytochromes (Huang *et al.*, 2016). Their composition includes not only phytochromes but also key transcriptional regulators like PAP5/HEMERA/pTAC12, which is required for photobody formation and photomorphogenesis (Chen *et al.*, 2010; Yoo *et al.*, 2019).

Here, we show first that PAP3 fused to a fluorescent tag is solely localized in plastids and second that the sporophytic-lethal mutant *pap3* display a good response to over-accumulation of the phytochrome-B-GFP fusion protein. We then propose to distinguish the existence of two albino syndromes within *paps* albino mutants according to the presence or absence of a predicted NLS within the coding sequence.

Materials and methods

Plant materials and growth conditions. *Arabidopsis thaliana* Columbia-0 (Col-0), the *pap3-1* T-DNA insertion mutant (CS16115), and the *pap3*-PHYB-GFP transgenic line were used. Seeds (~5000) were surface-sterilized in a 1.5 mL Eppendorf tube by two washes with 750 µL of 70% ethanol for 1 minute each, with gentle mixing by inversion and removal by pipetting. After ethanol removal, 60 µL of Domestos (commercial bleach, ~5% NaOCl) was added, and the seeds were mixed by tube inversion for 8 minutes. To preserve seed viability, total exposure to sterilizing agents did not exceed 20 minutes. The seeds were then washed three times with 1 mL of sterile water and placed on Murashige and Skoog (MS) medium, ensuring proper spacing. Seeds were then stratified at 4°C in darkness for 48 hours to synchronize germination. Growth conditions included two distinct light treatments: (1) continuous red light (660 nm/ ~ 8 $\mu mol.m^{-2}.s^{-1}$ photons) for 5 days and (2) continuous far-red light (730 nm) for 5 days.

Cellular lines. Transformation experiments utilized DH5α and One Shot™ TOP10 *Escherichia coli* competent cells stored at -80°C. The DH5α strain (F- Φ80lacZΔM15 Δ(lacZYA-argF) U169 recA1 endA1 hsdR17 (rk-, mk+) phoA supE44 thi-1 gyrA96 relA1 λ-) and the TOP10 strain (F- mcrA Δ(mrr-hsdRMS-mcrBC) Φ80lacZΔM15 lacX74 recA1 ara139 Δ(ara-leu)7697 galU galK rpsL (StrR) endA1 nupG) were used to maximize transformation efficiency.

Gentamicin-resistant pSOUP-containing electrocompetent *Agrobacterium tumefaciens* (strain C58 (rifR), Ti pMP90 (pTiC58DT-DNA) (gentR), pSOUP-p19 (tetR), nopaline) stored at -80°C was used for plant transformation.

Genetic materials: Vectors used included TOPO-BLUNT PCR cloning vectors (1 µL per topoisomerase reaction), binary vectors, and previously constructed plasmids (pQD11a, pCL02a9, pMT13, pBB330a*, pBB300, pBB301, pBB213, pCL23b, pKP20, pKP34). PCR-amplified inserts were obtained using specific primer pairs designed for cloning and verification purposes.

Plasmid DNA extraction: Plasmid DNA was extracted and purified using the ZymoPURE Plasmid Miniprep Kit. The procedure involved bacterial cell resuspension, alkaline lysis, and neutralization. Plasmid DNA was selectively bound to a silica matrix under high-salt conditions, followed by sequential washes to remove proteins, RNA, and other contaminants. Purified DNA was eluted in nuclease-free water and stored at -20°C.

DNA quantification: DNA concentration and purity were assessed using a NanoDrop™ 2000 spectrophotometer (Thermo Scientific). One microliter of nuclease-free water was used as a blank for baseline correction. DNA absorbance was measured at 260 nm, and purity was evaluated using the A260/A280 and A260/A230 ratios, where values >2 indicated minimal protein or RNA contamination.

Restriction enzyme digestion: Plasmid and PCR product digestions were performed using XhoI and BamHI for cloning, and NcoI, XbaI, HindIII, SacI, and SpeI for verification. Each reaction contained 2 µL of template DNA, 2 µL of 10X rCutSmart buffer, and the enzymes were used according to their unit definition on the concentration of vector and water in a total volume of 20 µL. Digestion was carried out at 37°C for 1 hour.

***Escherichia coli* and *Agrobacterium tumefaciens* transformation**. For *Escherichia coli* transformation, competent cells were prepared using 5xKMC buffer (500 mM KCl, 150 mM $CaCl_2$, 250 mM $MgCl_2$) prepared in advance, filter-sterilized (0.22 µm), and stored at -20°C. Transformation was performed by mixing 20 µl of 5xKMC, 70 µl of sterile water, and 10 µl of plasmid DNA. The mixture was added to the bacterial suspension and incubated on ice for 20 minutes, followed by a 10-minute incubation at room temperature. One milliliter of prewarmed LB or SOC medium was added, and the culture was incubated at 37°C for 1 hour with shaking. Transformed bacteria were plated on LB agar

supplemented with antibiotic and incubated overnight at 37°C. For *A. tumefaciens*, the transformation is done by electroporation because it is more efficient on large plasmids and Gram positive cells, such as *A. tumefaciens*. Five µL of vector were added to 50 µL of *A. tumefaciens* competent cells. These latter were then electrically shocked at 2500 V for 5 ms. Afterwards, the colonies were placed on LB agar medium with antibiotics such as: kanamycin, carbenicillin or spectinomycin. The Petri dishes were left overnight at 28°C under agitation and checked the next 2 days to assess the presence of resistant colonies.

Electrophoresis on agarose gel. The 1% agarose gel was prepared by adding 3 g of Roti®agarose to 300 mL of TAE 1X then warming while mixing periodically. For one gel, 25 mL of this solution was used alongside 2 µL of Red™ Safe 10,000X which was added in order to solidify the solution into a gel. Red™ Safe is a DNA intercalating agent which is added to allow DNA visualization under UV light emitted from the GelDoc™ BioRad. The solution was then poured into a chamber. After 20-30 minutes, the gel was immersed in TRIS Acetate EDTA 1% buffer, then the samples were injected with a loading dye (6X) into the wells. Thermo Scientific GeneRuler DNA Ladder Mix (5 µL) was also added into the wells to quantify the size of each band. The 1% agarose gel was submitted to an electric field at 110 V for 25 minutes in a solution of TAE 1X. After migration, it was analyzed under UV light (300 nm) with the Gel Doc™ BioRad.

Ligation. Ligation reactions were performed using a 3:1 molar ratio of insert to vector. This calculation was done with the following formula: (DNA mass/molecular weight)x$\mathcal{N}_{\text{Avogadro}}$. DNA mass is determined by comparison to known quantities of the ladder after an electrophoresis (Figure 6.b), the molecular weight is the number of base pairs multiplied by the weight of one base pair (660 g/mole), and Avogadro's number is a constant: 6.022×10^{23}. After determining the quantities of insert/vector that were being used, T4 DNA ligase was added with T4 buffer containing ATP in order to synthesize the phosphodiester bound. The samples were then left at room temperature for 4 hours.

Biolistic on onions. Also known as "particle bombardment", is a genetic transformation method done on plant cells where DNA is introduced into plant tissue, in our case onion epidermis, for transient expression. The process was the following:

- DNA mixture preparation: ~2,5 µg of gold beads in a final volume of 20 µL.
- Samples preparation with gold: 20 µL of Binding Buffer (Seashell™) is added into the DNA mixture. Preparation of 30 µL of gold (for 3 probes). 40 µL of Binding Buffer DNA mixed on the gold. Resuspended well by

pipetting and vortexing. After being kept on ice for 5 min, 70 µL of Precipitation Buffer is added. The supernatant is discarded after the suspension has been vortexed and kept on ice for 5-10 min. 500 µL of absolute Ethanol (100%) is added. Afterwards, the ethanol was removed and 30 µL of Ethanol 100% were added for pipetting the gold particles.

- Onion preparation: Fresh and turgid yellow onions were selected. Pieces were cut in such a way that the sample obtained had an intact epidermis. The annotation was done on the external face of it.
- Shooting: First, the pump has been turned on for vacuum, helium and PDS1000He then all of the required elements were placed (rupture disk, macro carrier, micro carrier, and stop grid). Furthermore, the vacuum switch was pressed until the gauge on the top of the gun read - 27 mm Hg, then the switch was put on "Hold". After that, the "Fire" switch was pressed and held until it popped at the rupture pressure. Finally, the vacuum was vented and the door opened. The onions were kept overnight in the dark before observation.

Primers. Primer sequences were designed using ApE (A Plasmid Editor; https://jorgensen.biology.utah.edu/wayned/ape), and used to generate PAP3 coding sequence fragments carrying silent point mutations that disrupt internal restriction enzyme sites without altering the encoded aminoacids. Those primers were also used to verify the presence of the modified PAP3 constructs in bacterial colonies via PCR.

Sequencing. To confirm the presence of the desired point mutations in the PAP3 coding sequence, plasmid DNA (15 µL at 100 ng·µL^{-1}) together with the corresponding primers was submitted to Eurofins Genomics (Ebersberg, Germany) for Sanger sequencing.

Results

Cloning PAP3

XhoI and BamHI are two restriction sites that were added using PCR at the beginning and end of the PAP3 coding sequence, because they are suitable for our cloning strategies. The problem is the presence of one more of each inside the coding sequence, meaning that some modifications had to be made in order to use available plasmids in the lab (Fig. 1A). Two point mutations were design so that the amino acid produced will not be changed, but the restriction sites would be disrupted. In the XhoI site, CTC was changed to CTT, both codons

encoding leucine, while in the BamHI site, ATC was changed to ATT, both encoding isoleucine (Fig. 1A. Those changes were made with specific primers, design in such a way that they would align to the template DNA even with those point mutations thanks to the high number of cytosine (C) and guanine (G) nucleotides at both ends.

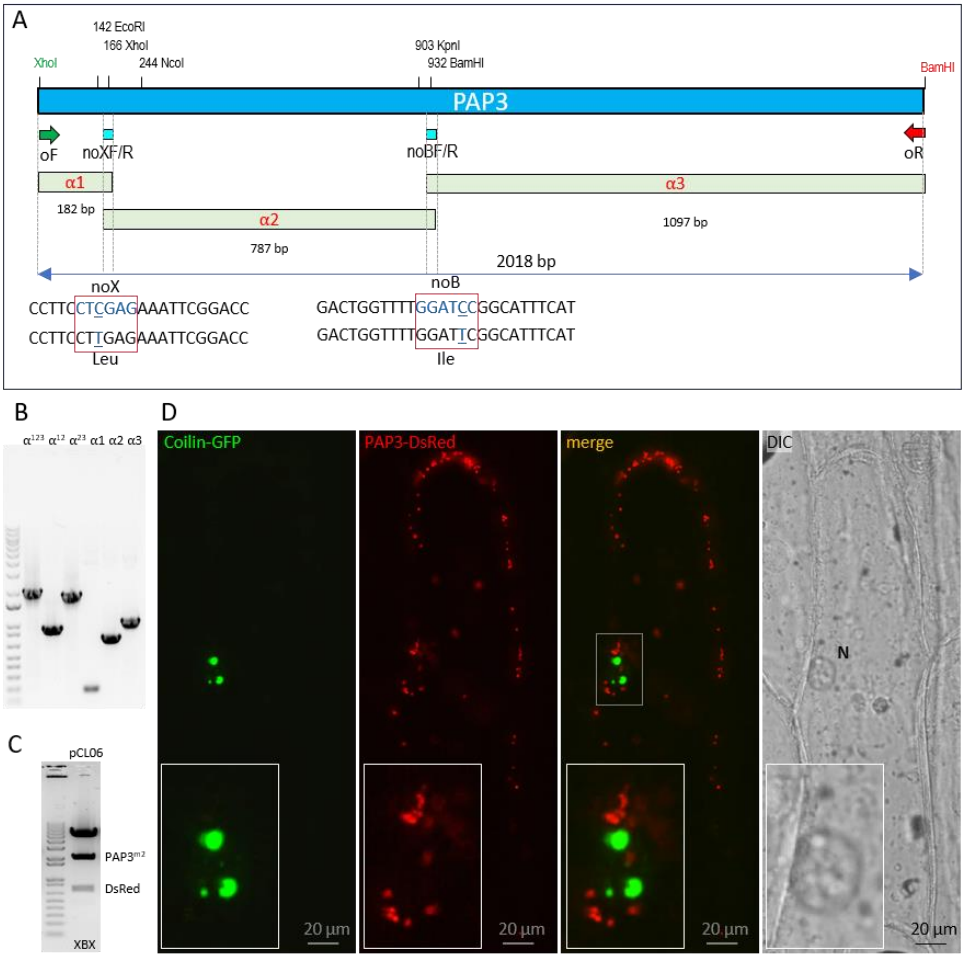

Figure 1. Cloning strategy and localization of PAP3 in the chloroplast. A. Map of the PAP3 coding sequence including restriction sites, the three α fragments derived from the PAP3 sequence, and location of primers. B. Phusion PCR and fragment extension PCR of α fragments. C. Enzyme digestion of pCL06 with XhoI/BamHI/XbaI. D. Subcellular localization of PAP3-DsRed compared to nuclear marker coilin-GFP in onion epidermal cells following biolistic transformation.

The PAP3 sequence was divided in three parts (α1, α2 and α3) in order to ensure a proper product with no XhoI/BamHI restriction sites within (Fig. 1B). The fragments were obtained with the corresponding primers in a Hot Start Phire PCR, and the final recombinant sequence was achieved via fragment extension PCR (Fig. 1B).

Red Fluorescent Protein (DsRed2) is a fluorescent marker that was added to PAP3 via cloning in order to continue the experiments in various directions. The resulting construct was verified with restriction enzymes for the presence of PAP3 and DsRed (Fig. 1C).

Localization of PAP3 in the chloroplast

Subcellular localization of PAP3 was done with biolistic transformation on epidermal onion cells using PAP3-DsRed (pCL06). Microscopy was employed to capture high-resolution fluorescence signals across multiple channels. Coilin-GFP fluorescent signal is restricted to the nucleus, confirming the nuclear compartment's spatial integrity (Fig. 1D). DsRed channel reveals discrete fluorescence exclusively within plastid-like structures, indicating robust localization of PAP3 to the chloroplast (Fig. 1D). Notably, no DsRed signal was observed in the nucleus. Merged image of both channels (Fig. 1D), highlighting the clear spatial segregation between PAP3-DsRed and coilin-GFP signals, and further supporting the absence of nuclear targeting for PAP3. Differential Interference Contrast image (DIC) delineates cellular boundaries and validates the structural context of the fluorescence signals (Fig. 1D).

PHYB-mediated light response

Stable overexpression of phytochrome PHYB-GFP (PBG) is known to mediate hypersensitivity of *Arabidopsis* seedlings to red light leading to a significant inhibition of hypocotyl elongation when compared to wild-type (Fig. 2A, 2B). After introducing PBG into *pap3* mutant background, this PBG effect remained the same, meaning that PAP3, as opposed to PAP8, does not play a role in the PHYB-mediated light response (Fig. 2B, 2C, 2D). This finding serves as evidence towards the difference in albino syndromes between PAPs with a single subcellular localization (PAP3 in chloroplast) and ones with dual localization (PAP8 in nucleus and chloroplast).

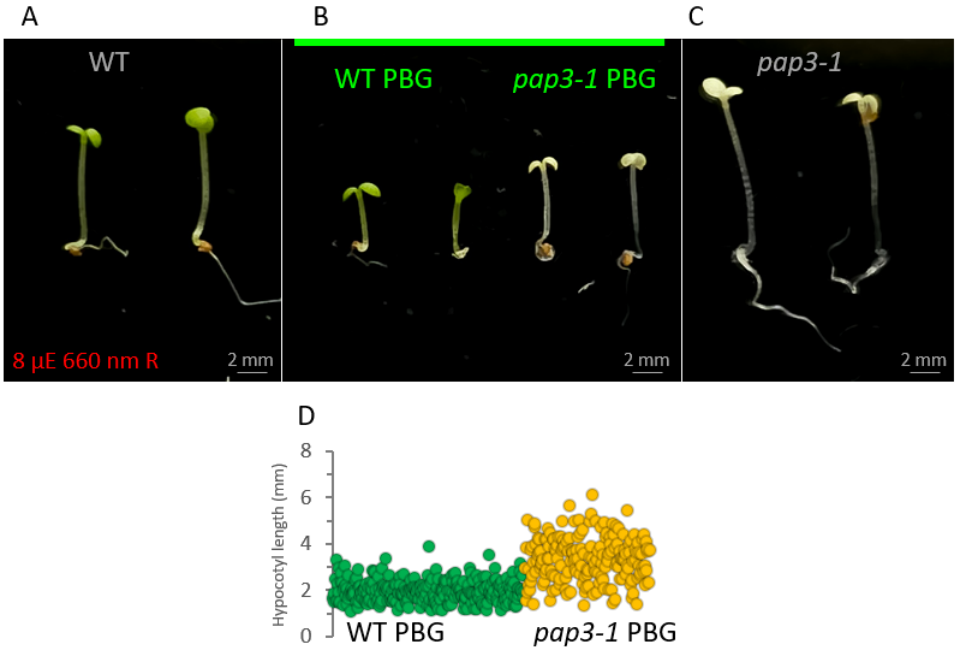

Figure 2. PAP3 is not essential for the PHYB-mediated light induction of photomorphogenesis. A-C. Phenotypes of given genotypes subjected to 5 days of illumination at 8 µmol m^{-2} s^{-1} 660-nm red light. D. Data analysis comparing the hypocotyl size between wild type and *pap3-1* mutant.

Photobody formation

Photobodies are dynamic subnuclear structures where activated phytochromes, particularly PHYB, accumulate in response to light. In wild-type *Arabidopsis thaliana* seedlings, active PHYB rapidly forms large, stable photobodies upon red light exposure, which correlates with robust transcriptional reprogramming and repression of hypocotyl elongation (Fig. 3A. Conversely, in *pap8* mutants, PHYB fails to form these large photobodies efficiently, remaining only small and numerous early photobodies. In contrast, PAP3 does not appear to share this functionality. In the *pap3* mutant background, photobody formation proceeds normally in the absence of PAP3 (Fig. 3B). The shape, number and dimensions are relatively the same when comparing *pap3* mutant to the WT, and the transition from early, small and numerous photobodies to late, big and few in number is not altered at all between the two, further distinguishing PAP3 from PAP8 in this context (Fig. 3B, 3C).

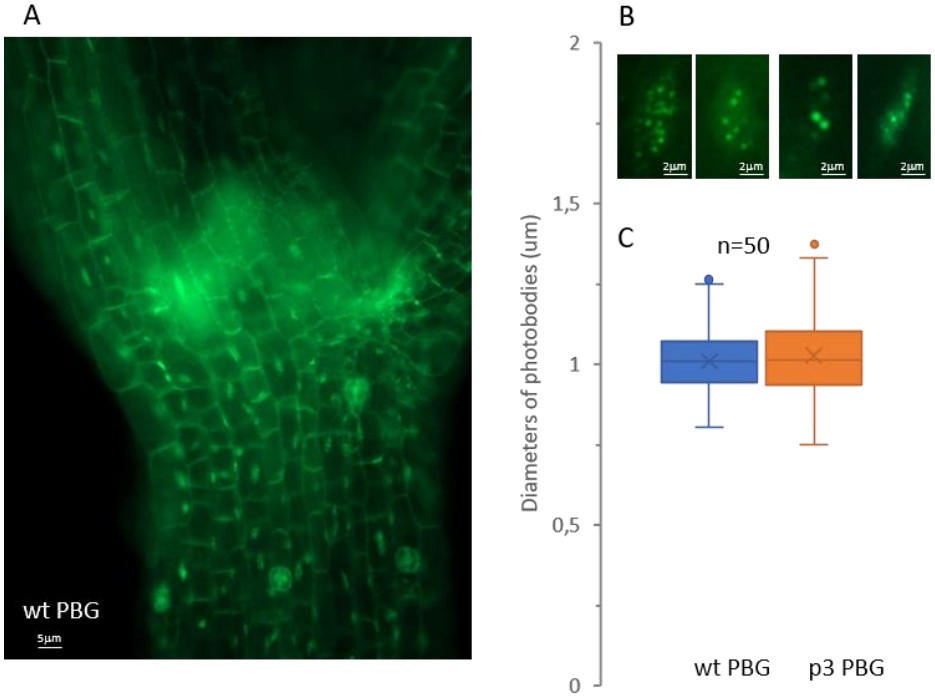

Figure 3. Photobody formation is not hindered in the *pap3-1* mutant. A. Whole-seedling image showing general GFP signal distribution across the plant. B. Accumulation of PBG observed under GFP excitation in the given genotypes (wt-PBG/*pap3-1* PBG) using epi-fluorescence microscopy. C. Data analysis of phodobodies size from the PBG and *pap3-1* PBG lines.

Discussion

Plastid gene expression in angiosperms relies on the plastid-encoded RNA polymerase (PEP) complex and its associated nuclear-encoded proteins called PAPs, several of which have been involved in plastid transcription and nuclear light signaling pathways. Previous studies showed that some PAPs, such as PAP8/pTAC6 and PAP5, display dual localization to plastids and the nucleus and play a role in coordinating chloroplast biogenesis with photomorphogenesis (Liebers *et al*., 2020; Liebers *et al*., 2022).

In this study, it is shown that PAP3/pTAC10 is exclusively localized to plastids and does not participate in PHYB-mediated light signaling pathway. Subcellular localization experiments revealed no detectable nuclear accumulation

of PAP3, in contrast to dually localized PAPs previously described in literature. This plastid-confined localization is consistent with earlier proteomic studies identifying PAP3 as a structural component of the transcriptionally active plastid chromosome (pTAC), rather than as a signaling factor involved in nucleus–plastid communication (Pfannschmidt *et al*., 2000; Steiner *et al*., 2011).

Functional analyses further support this distinction. While *pap8-1; PBG* exhibit defects in hypocotyl de-etiolation and impaired photobody formation under red light, *pap3-1; PBG* display normal PHYB nuclear body assembly and red light hypersensitivity. These observations indicate that PAP3 is not one of the main actors in the PHYB-mediated light signaliing pathway, reinforcing the idea that its function is confined to the plastid compartment (Kindgren and Strand, 2015).

Together, these results support a functional distinction among PAPs based on their subcellular localization. Dually localized PAPs have been shown to play a role in both plastid gene expression and nuclear light-regulated processes, whereas plastid-confined PAPs, such as PAP3, appear to function primarily within the plastid transcriptional machinery. Therefore, the absence of PAP3 does not impair PHYB-mediated light signaling pathway, indicating that its function is not required for photobody formation or red light–dependent photomorphogenic responses.

This distinction refines current models of plastid–nucleus communication by emphasizing that not all components of the PEP complex contribute to retrograde signaling. Instead, the regulatory scope of individual PAPs appears to be tightly linked to their subcellular localization and molecular function within the PEP complex.

Conclusions

This study identifies PAP3/pTAC10 as a plastid-confined component of the plastid-encoded RNA polymerase complex. Fluorescent localization analyses demonstrate that PAP3 localizes exclusively to plastids and does not enter the nucleus.

Functional characterization of the *Arabidopsis pap3-1* mutant shows that PAP3 is not required for PHYB-mediated light signaling pathway, hypocotyl de-etiolation, or photobody formation. These findings distinguish PAP3 from dually localized PAPs, such as PAP8, which are involved in both plastid transcription and nuclear light signaling.

Overall, these results support a functional classification of PEP-associated proteins based on subcellular localization, in which plastid-confined PAPs primarily affect chloroplast biogenesis, whereas dually localized PAPs integrate plastid development with nuclear photomorphogenic pathways.

References

Archibald, J. M. (2015). Endosymbiosis and eukaryotic cell evolution. *Current Biology*, *25*(19), R911–R921. https://doi.org/10.1016/j.cub.2015.07.055

Bock, R., & Timmis, J. N. (2008). Reconstructing evolution: Gene transfer from plastids to the nucleus. *BioEssays*, *30*(6), 556–566. https://doi.org/10.1002/bies.20761

Börner, T., Aleynikova, A. Y., Zubo, Y. O., & Kusnetsov, V. V. (2015). Chloroplast RNA polymerases: Role in chloroplast biogenesis. *Biochimica et Biophysica Acta (BBA) - Bioenergetics*, *1847(9)*, 761–769. https://doi.org/10.1016/j.bbabio.2015.02.004

Cappadocia, L., Maréchal, A., Parent, J.-S., Lepage, étienne, Sygusch, J., & Brisson, N. (2010). Crystal Structures of DNA-Whirly Complexes and Their Role in *Arabidopsis* Organelle Genome Repair. *The Plant Cell*, *22*(6), 1849–1867. https://doi.org/10.1105/tpc.109.071399

Chan, C. X. & Bhattacharya, D*.* (2010*). The Origin of Plastids. Nature Education 3(9):84.*

Chen, M., Galvão, R. M., Li, M., Burger, B., Bugea, J., Bolado, J., & Chory, J. (2010). *Arabidopsis* HEMERA/pTAC12 initiates photomorphogenesis by phytochromes. *Cell*, *141*(7), 1230–1240. https://doi.org/10.1016/j.cell.2010.05.007

Chen, M., Schwab, R., & Chory, J. (2003). Characterization of the requirements for localization of phytochrome B to nuclear bodies. *Proceedings of the National Academy of Sciences*, *100*(24), 14493–14498. https://doi.org/10.1073/pnas.1935989100

Choi, H., Yi, T., & Ha, S.-H. (2021). Diversity of plastid types and their interconversions. *Frontiers in Plant Science*, *12*. https://doi.org/10.3389/fpls.2021.692024

Huang, H., Yoo, C. Y., Bindbeutel, R., Goldsworthy, J., Tielking, A., Alvarez, S., Naldrett, M. J., Evans, B. S., Chen, M., & Nusinow, D. A. (2016). PCH1 integrates circadian and light-signaling pathways to control photoperiod-responsive growth in *Arabidopsis*. *eLife*, *5*, e13292. https://doi.org/10.7554/eLife.13292

Kindgren, P., & Strand, Å. (2015). Chloroplast transcription, untangling the Gordian Knot. *New Phytologist*, *206*(3), 889–891. https://doi.org/10.1111/nph.13388

Liebers, M., Cozzi, C., Uecker, F., Chambon, L., Blanvillain, R., & Pfannschmidt, T. (2022). Biogenic signals from plastids and their role in chloroplast development. *Journal of Experimental Botany*, *73*(21), 7105–7125. https://doi.org/10.1093/jxb/erac344

Liebers, M., Gillet, F., Israel, A., Pounot, K., Chambon, L., Chieb, M., Chevalier, F., Ruedas, R., Favier, A., Gans, P., Boeri Erba, E., Cobessi, D., Pfannschmidt, T., & Blanvillain, R. (2020). Nucleo-plastidic PAP8/pTAC6 couples chloroplast formation with photomorphogenesis. *The EMBO Journal*, *39*(22), e104941. https://doi.org/10.15252/embj.2020104941

Pfannschmidt, T., Ogrzewalla, K., Baginsky, S., Sickmann, A., Meyer, H. E., & Link, G. (2000). The multisubunit chloroplast RNA polymerase A from mustard (*Sinapis alba*). *European Journal of Biochemistry*, *267*(1), 253–261. https://doi.org/10.1046/j.1432-1327.2000.00991.x

Steiner, S., Schröter, Y., Pfalz, J., & Pfannschmidt, T. (2011). Identification of essential subunits in the plastid-encoded RNA polymerase complex reveals building blocks for proper plastid development1[C][W][OA]. *Plant Physiology*, *157*(3), 1043–1055. https://doi.org/10.1104/pp.111.184515

Yoo, C. Y., Williams, D., & Chen, M. (2019). Quantitative analysis of photobodies. In A. Hiltbrunner (Ed.), *Phytochromes* (Vol. 2026, pp. 135–141). Springer New York. https://doi.org/10.1007/978-1-4939-9612-4_10